

Reduction of Elevated Proton Leak Rejuvenates Mitochondria in the Aged Cardiomyocyte

Huilian Zhang¹, Nathan N. Alder², Wang Wang^{1,3}, Hazel Szeto⁴, David J. Marcinek⁵, Peter S. Rabinovitch^{1*}

1. Department of Pathology, University of Washington, Seattle, WA 98195, USA
2. Department of Molecular and Cell Biology, University of Connecticut, Storrs, CT 06269, USA
3. Mitochondria and Metabolism Center, Department of Anesthesiology and Pain Medicine, University of Washington, Seattle, WA 98109, USA
4. Social Profit Network Research Lab, Alexandria LaunchLabs, New York, NY 10016, USA.
5. Department of Radiology, University of Washington, Seattle, WA 98105, USA

*correspondence: petersr@uw.edu

Abstract

Aging-associated diseases, including cardiac dysfunction, are increasingly common in the population. However, the mechanisms of physiologic aging in general, and cardiac aging in particular, remain poorly understood. While effective medical interventions are available for some kinds of heart failure, one age-related impairment, diastolic dysfunction in Heart Failure with Preserved Ejection Fraction (HFpEF) is lacking a clinically effective treatment. Using the model of naturally aging mice and rats, we show direct evidence of increased proton leak in the aged heart mitochondria. Moreover, we identified ANT1 as mediating the increased proton permeability of old cardiomyocytes. Most importantly, the tetra-peptide drug SS-31 (elamipretide) prevents age-related excess proton entry, decreases the mitochondrial flash activity and mitochondrial permeability transition pore (mPTP) opening and rejuvenates mitochondrial function by direct association with ANT1 and the mitochondrial ATP synthasome. Our results uncover a novel mechanism of age-related cardiac dysfunction and elucidate how SS-31 is able to reverse this clinically important complication of cardiac aging.

Significance

Aging is the greatest risk factor for cardiac dysfunction, including Heart Failure with Preserved Ejection Fraction (HFpEF). Unfortunately, the mechanisms of cardiac aging remain elusive, and there are no effective pharmacologic therapies for HFpEF. Here, we show direct evidence of increased proton leak in aged cardiac mitochondria and have identified ANT1 as mediating the increased proton permeability of old cardiomyocytes. Moreover, the mitochondrial-targeted tetra-peptide SS-31 (elamipretide) prevents the age-related excess proton entry and rejuvenates mitochondrial function by direct association with ANT1 and the mitochondrial ATP synthasome, resulting in alleviation of diastolic dysfunction in old mice. Our results unmask a novel mechanism of cardiac aging and elucidate how SS-31 reverses this clinically important complication of aging.

43 Introduction

44 Mitochondria are both the primary source of organismal energy and the major source of cellular
45 reactive oxygen species (ROS) and oxidative stress during aging (1). Aged cardiac
46 mitochondria are functionally changed in redox balance and are deficient in ATP production (2).
47 Numerous reported studies have focused on redox stress and ROS production in aging (1).
48 However, in its simplistic form, the free radical theory of aging has become severely challenged
49 (3).

50 While more attention has been placed on mitochondrial electron leak and consequent free
51 radical generation, proton leak is a highly significant aspect of mitochondrial energetics, as it
52 accounts for more than 20% of oxygen consumption in the liver (4) and 35% to 50% of that in
53 muscle in the resting state (5). There are two types of proton leak in the mitochondria: 1)
54 constitutive, basal proton leak, and 2) inducible, regulated proton leak, including that mediated
55 by uncoupling proteins (UCPs) (6). In skeletal muscle, a majority of basal proton conductance
56 has been attributed to adenine nucleotide translocase (ANT) (7). Although, aging-related
57 increased mitochondrial proton leak was detected in the mouse heart, kidney and liver by
58 indirect measurement of oxygen consumption in isolated mitochondria (8, 9), direct evidence of
59 functional impact remains to be further investigated. Moreover, the exact site and underlying
60 mechanisms responsible for aging-related mitochondrial proton leak are unclear.

61 SS-31 (elamipretide), a tetrapeptide (D-Arg-2',6'-dimethyltyrosine-Lys-Phe-NH₂), binds to
62 cardiolipin-containing membranes (10) and improves cristae curvature (11). Prevention of
63 cytochrome *c* peroxidase activity and release has been proposed as its major basis of activity
64 (11, 12). SS-31 is highly effective in increasing resistance to a broad range of diseases,
65 including heart ischemia reperfusion injury (13, 14), heart failure (15), neurodegenerative
66 disease (16) and metabolic syndrome (17). In aged mice, SS-31 ameliorates kidney
67 glomerulopathy (18) and brain oxidative stress (19) and has shown beneficial effects on skeletal
68 muscle performance (20). We have recently shown that administration of SS-31 to 24 month old
69 mice for 8 weeks reverses the age-related decline in diastolic function, increasing the E/A from
70 just above 1.0 to 1.22, restoring this parameter 35% towards that of young (5 month old) mice
71 (21). However how SS-31 benefits and protects aged cardiac cells remains unclear.

72 In this report we investigated the effect and underlying mechanism of action of SS-31 on aged
73 cardiomyocytes, especially on the mitochondrial proton leak. Using the naturally aged rodent
74 model we provided direct evidence of increased proton leak as the primary energetic change in
75 aged mitochondria. We further show that the inner membrane protein ANT1 mediates the
76 augmented proton entry in the old mitochondria. Most significantly, we demonstrate that SS-31
77 prevents the proton entry and rejuvenates mitochondrial function through direct association with
78 ANT1 and stabilization of the ATP synthasome.

79 Results

80 **SS-31 alleviates the excessive mitochondrial proton leak in old cardiomyocytes.** To
81 examine whether SS-31 restores aging mitochondrial function, we applied the Seahorse
82 mitochondrial stress assay to intact primary cardiomyocytes. The Seahorse Assay revealed
83 higher mitochondrial basal respiration in cells from old mice than that in young mouse cells (Fig
84 1A, C); however, the maximal respiratory rate was not significantly different (Fig 1A, D). The
85 increased basal respiration was attributable to a higher proton leak in old cardiomyocytes ($165 \pm$
86 15 in 24 month vs 86 ± 8 in young, pmol/min/800cells, $n=11-33$, $p<0.05$) (Fig. 1A, B). Acute *in*
87 *vitro* treatment of isolated old cardiomyocytes with SS-31 (100 nM, 1 μ M, or 10 μ M for 2 hrs),

88 caused reduced mitochondrial basal respiration (Fig. 1A, C and Fig. S1), shifting their
89 respiratory pattern to a more youthful state. The respiratory control ratio (RCR) was also
90 increased in treated aged cardiomyocytes relative to untreated aged cells (Fig. 1E), which was
91 entirely explained by reduced proton leakage (Fig. 1B). These results indicate that SS-31
92 directly protects aging cardiac energetics through rapid rejuvenation of mitochondrial respiration
93 in cardiomyocytes, and in particular, by reducing proton leak.

94 **SS-31 restores the resistance to external pH gradient stress in old cardiomyocytes.** To
95 directly investigate the reduction of mitochondrial proton leak in old cardiomyocytes by SS-31,
96 we expressed the protein mt-cpYFP, a mitochondrial matrix-targeted indicator that was thought
97 to be sensitive to superoxide (22) but turns out to be more sensitive to pH change (23-25) (Fig.
98 S2). Taking advantage of the pH sensitive character of mt-cpYFP, we developed a novel
99 protocol to evaluate mitochondrial proton leak by exposing mitochondria to a pH gradient stress
100 in saponin permeabilized, mt-cpYFP expressing cardiomyocytes (Fig. 2A). The drop in mt-
101 cpYFP 488/405 ratio is due to proton leak through the mitochondrial inner membrane into the
102 mitochondrial matrix. To evaluate the physical properties of the mitochondrial inner membrane
103 in the absence of mitochondrial activity, we permeabilized the cardiomyocytes in a buffer that
104 contained no substrates, ATP, or ADP. We found that aging reduced cardiomyocyte
105 mitochondrial resistance to a proton gradient stress (Fig. 2A). More importantly, we found 10 μ M
106 SS-31 treatment *in vitro* restored cardiomyocyte mitochondrial inner membrane resistance to the
107 pH gradient stress in the aged cardiomyocytes (Fig. 2A). SS-31 treatment largely prevented the
108 decline in matrix pH of old cells after the external pH was reduced to 5.3 (Fig. 2B, S3) and
109 slowed the rate of cpYFP 488/405 change after pH 6.9 (Fig. 2C, S4). To further evaluate the
110 kinetics of SS-31 effect on mitochondrial proton permeability, we analyzed cpYFP fluorescence
111 ratios at various times after exposure of the saponin treated cardiomyocytes to 10 μ M SS-31.
112 SS-31 protection of on the mitochondrial matrix proton entry became significant and near
113 maximal after 7-10 minutes of SS-31 treatment (Fig. 2D). We examined the dose effect of SS-
114 31 on proton permeability and found near-maximal effects at 100 nM SS-31 (Fig. 2E). In
115 summary, this is the first direct evidence that aging increases mitochondrial inner membrane
116 proton permeability in aged cardiomyocytes and that SS-31 protects cardiomyocytes from this
117 proton leak.

118 **ANT1 inhibitors restore resistance of old cardiomyocytes to proton leak.** In search of the
119 source of the uncoupled proton leak in the aged cells, we examined possible involvement of
120 proton leakage through ATPase and mitochondrial uncoupling proteins (UCPs). The ATPase
121 inhibitor Oligomycin A failed to inhibit the proton leak in pH challenged permeabilized aged cells
122 (Fig. 3A, B). Levels of UCP2, which is the dominant isoform of UCPs in the heart, do not change
123 with in age in hearts (Fig. S5). Genipin, an inhibitor of UCP2, showed no effect on the proton
124 leak in permeabilized aged cells (Fig 3A, B). These results suggest that the ATPase and UCP2
125 may not be the source of the excess proton leak in the aged hearts.

126 Recently, the inner membrane protein ANT1 (also called AAC) was identified as the major site
127 of proton leak in mitochondria of multiple tissues (26), and was shown to contribute to the
128 majority of the proton leak in muscle cells (7). Treatment of old cardiomyocytes with either the
129 ANT1 inhibitor bongkreic acid (BKA) (27) or carboxyatractyloside (CAT) (28) completely
130 suppressed the excess proton leak in the Seahorse assay, though unlike SS-31, they also
131 decreased the maximal respiratory rate and failed to enhance the RCR (Fig 1B, C, E), which is
132 consistent with the effect seen in the ANT triple knockout model (29). We treated permeabilized
133 old cardiomyocytes with the ANT1 inhibitors and examined the mt-cpYFP response to an
134 external pH gradient using the protocol described above. BKA suppressed the proton leak in old
135 cardiomyocytes, evidenced by the preserved 488/405 ratio at pH 5.3 and a slower 488/405 ratio

136 decrease at pH 6.9 (Fig. 3A, B). Similar inhibition was found with CAT treatment (Fig. 3A, B).
137 Taken together, these data implicate ANT1 as the major site of proton leak in aging hearts.

138 **SS-31 attenuates the excessive mitochondrial flash (mitoflash) activity of aged**
139 **cardiomyocytes, while normalizing membrane potential and ROS.** The mitoflash (22, 30-
140 34), is triggered by nanodomain proton influx into the mitochondrial matrix (35). Thus, we
141 wondered whether the increased proton leak in the old cells triggered excessive mitoflash
142 activity. We evaluated mitoflash activity in isolated young and old rat cardiomyocytes using the
143 indicator mt-cpYFP, as established in the previous studies noted above. The mitochondrial
144 mitoflash activity in the cells from old (26 mo) cardiomyocytes was higher than that of young (5
145 mo) cells (2.8 ± 0.3 in old vs 1.4 ± 0.2 , /1000 μm^2 /100s in young cells, n=28-88, p<0.05).
146 Confirming this, we detected an increase in mitoflash activity in Langendorff perfused intact
147 aged hearts from mt-cpYFP transgenic mice (Fig. S6). 1 hour treatment with SS-31 normalized
148 the mitoflash activity in old cells to the young cell level (Fig. 4D). Moreover, the mitochondrial
149 ANT1 inhibitors BKA and CAT showed super-suppression of the flash activity, reducing this
150 frequency to half of that of young cells (Fig. 4D). These data support the notion that proton leak
151 from ANT1 triggers the mitoflash in cardiomyocytes and is responsible for the excess mitoflash
152 activity of old cells. Moreover, the mitochondrial membrane potential, which is lower in old
153 cardiomyocytes, is restored to youthful levels by SS-31 treatment (Fig. 4E). Also, SS-31
154 reduced ROS production in the aged cardiomyocytes (Fig. 4F). Thus, the reduction of
155 mitochondrial proton leak by SS-31 is accompanied by a more youthful membrane potential and
156 dynamic function (mitoflash), as well as less oxidative stress.

157 **SS-31 reverses increased mPTP opening in aged cardiomyocytes.** Due to the close link
158 previously established between the mitoflash and mitochondrial permeability transition pore
159 (mPTP) opening (33), we evaluated mPTP activity by the photon-triggered mPTP opening
160 protocol (Fig. 5A) (36). Consistent with previous reports in isolated mitochondria (37), we found
161 that the time to mPTP opening is decreased in intact old cardiomyocytes (Fig. 5B). SS-31 and
162 the ANT1 inhibitor BKA, which stabilizes the ANT1 in the m-state open towards the
163 mitochondrial matrix, both protect the aging-increased mitochondrial mPTP opening rate (Fig.
164 5B), consistent with previous observations that BKA prevents the onset of the permeability
165 transition (38). The ANT1 inhibitor CAT, which stabilizes ANT1 in the c-state open toward the
166 cytosol, failed to prevent the rapid opening of the mPTP in old cells (Fig. 5B), consistent with
167 previous observations that it facilitates mPTP opening (38). These data indicate that SS-31
168 decreases mPTP opening in old cardiomyocytes.

169 **SS-31 associates directly with ANT1 and the ATP synthasome.** To further investigate the
170 mechanism of SS-31 protection of the proton leak, we used biotinylated SS-31 to evaluate
171 whether SS-31 directly interacts with the ANT1 protein. Hearts were disrupted by douncing,
172 after a low speed spin to remove fragments, mitochondria were collected by high speed spin
173 and disrupted in digitonin, to create lipid rafts containing their associated proteins, a protocol
174 commonly used to prepare mitochondrial supercomplexes (39). This preparation was incubated
175 with SS-31-biotin or biotin only, followed by incubation with streptavidin beads. After washing,
176 the bead-bound fraction was eluted with excess SS-31 and analyzed by Western blotting.
177 Biotin-SS-31 pulled down ANT1, and free SS-31 competed with the biotin-SS-31 binding to
178 ANT1 (Fig. 6A, B). Most notably, both BKA and CAT inhibited binding of biotin-SS-31 to ANT1
179 (Fig. 6A, B). This competition was observed even at BKA and CAT concentrations in the tens of
180 nanomolar range, which is similar to their reported K_d of binding to ANT1 (40) (data not
181 shown). Biotin-SS-31 pulldown of ANT1 was not inhibited by Genipin or Oligomycin A (Fig. 6A,
182 B). These data indicate that SS-31 associates closely with the ANT1 protein. Moreover, native
183 gel and ATPase blot analysis showed that SS-31 stabilized the ATP synthasome, of which

184 ANT1 and ATPase are critical members (41) (Fig. 6D, E and S7). However, SS-31 treatment did
185 not produce a detectable increase in mitochondrial complex proteins by Coomassie blue
186 staining (Fig. 6C). Taken together, these data suggest that SS-31 interacts directly with ANT1
187 and stabilizes the ATP synthasome in old cardiomyocytes.

188 **Discussion:**

189 In this report we have shown direct evidence of increased proton leak in the aged mitochondria
190 as a primary energetic disturbance and evidence that the increased proton entry in old
191 cardiomyocytes takes place through ANT1. Moreover, we demonstrated that SS-31 prevents
192 the proton entry to the mitochondrial matrix and rejuvenates mitochondrial function through
193 direct interaction with ANT1 and stabilization of the ATP synthasome. During aging, the
194 pathological augmented and sustained basal proton leak burdens the mitochondrial work load,
195 resulting in a decline in respiratory efficiency. Blocking this pathological proton leak induced by
196 aging benefits the mitochondria and the heart (Fig. 7). We suggest that the restoration of aged
197 mitochondrial function that is conferred by SS-31 is directly attributable to this effect. However,
198 the resulting enhancement in diastolic function is likely to require downstream changes, as the
199 functional benefit took up to 8 weeks to reach full effect, and required post-translational
200 modifications of contractile protein elements (21). It is increasingly recognized that mitochondrial
201 function, including redox status and energetics, has far-reaching effects, including epigenetic
202 alterations and post-translational modifications (42).

203 ANT1 appears to mediate the pathological mitochondrial proton leak in the aged mouse heart.
204 Although an increased mitochondrial proton leak in the aged heart was previously suggested by
205 indirect oxygen consumption measurement (9), the site of this augmented proton leak in aging
206 mitochondria has remained a puzzle. We directly evaluated the proton leak using the
207 mitochondrial matrix targeted pH indicator (mt-cpYFP) and provide evidence that implicates
208 ANT1, the ATP/ADP translocator, as responsible for the pathologically increased proton leak in
209 aged cardiomyocytes. This does not necessarily implicate the ADP/ATP translocase mechanism
210 itself in the proton leak, as in the unenergetic state in which we examined the mitochondrial pH
211 resistance, there would be no ADP/ATP transport activity. Our result is, however, supported by
212 a recent report that proton transport is an integral function of ANT1 (26). Because the ANT1
213 protein level is not increased in the aged heart (it is, in fact, mildly but significantly decreased,
214 Fig. S5), the aging-augmented proton leak through ANT1 must be through altered transport
215 activity or conformational change. Both the inhibitors of BKA (locking ANT1 in m-state (27)) and
216 CAT (locking ANT1 in c-state (28)) suppressed the proton leak in the aged cardiomyocytes,
217 suggesting that constraining the conformational state in either position, or otherwise blocking
218 the proton pore reduces ANT1 proton translocation.

219 Most interestingly, for the first time, we showed that a novel drug, SS-31 (elamipretide), now in
220 clinical trials, prevents the augmented mitochondrial proton leak, rejuvenates mitochondria
221 function and reverses aging-related cardiac dysfunction. Mechanistically, we found that SS-31
222 directly interacts with ANT1 and stabilizes formation of the ATP synthasome. This would seem
223 surprising, given the prior belief that SS-31 affects mitochondria via binding to cardiolipin.
224 However, the notion that SS-31 prevents the proton leak by direct interaction at the pore
225 “pocket” of ANT1 is supported by recent observations based on cross-linking “interactome”
226 mass-spectroscopy that showed that SS-31 is in intimate proximity to two lysine amino acid
227 residues in the water filled cavity of the ANT1 protein (43). Moreover, the cross-linking data
228 suggested that this interaction may have structural consequences and may stabilize the m-state
229 of ANT1. Our observation that both BKA and CAT blocked the SS-31 interaction with ANT1
230 suggests that SS-31 interacts with ANT1 independent of the ANT1 face to m-state (matrix

231 facing) or c-state (cytoplasmic-facing). It has recently been shown that SS-31 alters surface
232 electrostatic properties of the mitochondrial inner membrane (44). The consequences of this
233 effect could include alteration of the channel ion gating properties of the ANT and/or promotion
234 of supercomplex and ATP synthasome complex stability. Thus, we do not wish to convey the
235 impression that SS-31 effects only ANT1, as this is certainly not the case (Supplemental Figure
236 8, and reference (43)). Stabilization of mitochondrial supercomplexes and the synthasome could
237 directly contribute to the enhanced mitochondrial respiratory efficiency that is seen in muscle of
238 SS-31 treated old animals (20) and the improvement in performance of humans with primary
239 mitochondrial myopathy (45) that forms the basis of an ongoing Phase III Clinical trial
240 (NCT03323749).

241 The restoration of membrane potential by SS-31 the old mitochondria (Fig. 4E) can be attributed
242 to the suppression of proton leak. However, SS-31 also decreased ROS production (Fig. 4F) in
243 the aged cardiomyocytes. It is unclear if the reduced ROS production is associated with
244 modification of the ANT1 shown here or through a parallel mechanism. Blocking this
245 pathological proton leak induced by aging will benefit the mitochondria and the heart. This is not
246 in conflict with the “uncoupling to survive hypothesis”, which arises from the positive correlations
247 between increase proton leak, reduced ROS and increased lifespan (46). This reduced ROS
248 production is interpreted as resulting from decreased electromotive force and consequent
249 reduced electron leak during transport through the respiratory chain. However, SS-31 through
250 its interaction with cardiolipin, abundant in the inner membrane, can improve the efficiency of
251 electron transfer, especially by its known interaction with the heme group of cytochrome c (11,
252 12), thereby reducing ROS production, even as the aged mitochondrial membrane potential is
253 increased. Thus, our data support the conclusion that SS-31 interaction with multiple inner
254 membrane proteins enhances the performance of multiple facets of respiratory mechanics.

255 In summary, our study reveals that ANT1 is responsible for the elevated proton leak in old
256 cardiomyocytes and that SS-31 directly interacts with ANT1, preventing the proton leak and
257 rejuvenating mitochondrial function in the aged cardiomyocytes. The improved mitochondrial
258 function leads to complex secondary changes to effect enhanced diastolic function in the aged
259 heart. These findings provide a novel insight for better understanding of the mechanisms of
260 cardiac aging and establish the novel concept that decreasing the pathological proton leak in
261 the aging heart restores mitochondrial function, ultimately reversing cardiac dysfunction in
262 aging.

263 **Methods:**

264 **Animals.** All the animal procedures were approved by the Institutional Animal Care and Use
265 Committee at the University of Washington and conform to the NIH guidelines (Guide for the
266 care and use of laboratory animals). Young (4-6 month-old) and aged (24-26 month-old)
267 C57BL/6 mice (Charles River colony) and F344 rats were obtained from the National Institute of
268 Aging Rodent Resource. The mt-cpYFP transgenic C57BL/6 mice were housed until reaching
269 the age described.

270 **Isolation of adult mouse and rat cardiomyocytes.** Single ventricular myocytes were
271 enzymatically isolated from mouse and rat hearts as described previously (47, 48). The rod
272 shaped cardiomyocytes were collected by allowing cells settle down and adhere to laminin
273 coated 24 well Seahorse plates for intact cell oxygen consumption test or to glass coverslips for
274 confocal imaging.

275 **Seahorse Assay.** The XF24e Extracellular Flux Analyzer (Seahorse Bioscience) was used for
276 measuring oxygen consumption in intact cardiomyocyte, with XF assay medium containing 5
277 mM glucose and 1 mM pyruvate. Oligomycin A (OA, 2.5 μ M), carbonyl cyanide-p-
278 trifluoromethoxyphenylhydrazone (FCCP, 1 μ M), and antimycin A (AA, 2.5 μ M) plus 1 μ M
279 rotenone (Rot) were added in three sequential injections. The RCR was measured or calculated
280 by maximal respiration divided by basal respiration.

281 **Confocal imaging.** We used a Zeiss 510 (Zeiss, Germany) or Leica SP8 (Leica, Germany) for
282 confocal imaging at room temperature. The cells were placed in modified Tyrode's solution (in
283 mM: 138 NaCl, 0.5 KCl, 20 HEPES, 1.2 MgSO₄, 1.2 KH₂PO₄, 5 Glucose, 1 CaCl₂, pH 7.4). For
284 mitochondrial flashes, mt-cpYFP expressing cells were exposed to alternating excitation at 405
285 and 488 nm and emission collected at >505 nm. Time-lapse 2D images were collected at a rate
286 of 1 s per frame. For mitochondrial superoxide quantitation, we used the ratio of MitoSOX Red
287 (5 μ M, excited at 540 nm with emission collected at > 560 nm) to mitoTracker Green (200 nM,
288 excited at 488 nm and emission collected at 505-530 nm). For mitochondrial membrane
289 potential measurement, JC-1 was excited at 488 nm and emission collected at 510-545 nm and
290 570-650 nm. For photon triggered mPTP opening, the cells were loaded with 120 nM
291 Tetramethylrhodamine methyl ester (TMRM) and line scanned at 1 Hz as described previously
292 (36).

293 **Cell permeabilization and pH stress.** Rat cardiomyocytes were cultured with mt-cpYFP
294 adenovirus (34) for 3 days in M199 medium. After incubation in Ca²⁺-free Tyrode's solution for
295 30 min, the medium was changed to a solution of 100 mM potassium aspartate, 20 mM KCl, 10
296 mM glutathione, 10 mM KH₂PO₄, 0.1 mM EGTA, 8% dextran 40,000, pH 7.5, with 50 μ g/ml
297 saponin for 30 s and then maintained in saponin-free internal solution (49). The pH of the
298 solution containing the permeabilized cells was then progressively lowered by addition of HCl in
299 quantities previously titrated to result in pH 7.3, 6.9, 5.3, and 4.5, with 8 min between each step.
300 The permeabilized cells were excited using same settings as for mt-cpYFP above, but using a
301 time-lapse of 6 s per frame. The ratio of emission fluorescence at 488 nm from 405 nm
302 excitation indicated the mitochondrial pH change (23) and was normalized to a starting (pH 7.5)
303 arbitrary value of 1.0, so as to normalize differences due to variability of the intensity of laser
304 excitation and emission collection between different experiments.

305 **Western blots.** Heart tissue was lysed with RIPA buffer containing a protease inhibitor cocktail
306 (50). Protein samples were denatured and separated via NuPAGE Bis-Tris gel, and transferred
307 to PVDF membranes. The blots were probed with primary antibodies: ANT1 (Abcam, ab102032,

308 1:3000), UCP2 (Cell signaling technology, 89326S, 1:2000) followed by appropriate secondary
309 antibodies.

310 **Biotin-SS-31 pulldown and Blot Analysis.** Hearts were chunked and dounce homogenized in
311 mitochondrial isolation buffer (MIB, in mM: 300 sucrose, 10 Na-HEPES, 0.200 EDTA, pH 7.4)
312 and centrifuged at 800 g for 10 min. The supernatants were centrifuged at 8000 g for 15 min to
313 purify mitochondria. Digitonin was added to the mitochondria at a ratio of Digitonin : protein = 6
314 :1 to break down the membrane system. Treatment drugs were added 30 min before addition of
315 10 μ M biotin-SS-31 (Biotin-D-Arg-dimethyl Tyr-Lys-Phe-NH₂) or biotin control (Thermo,
316 B20656). Streptavidin Agarose beads (Thermo, 20349) were added and incubated 2 hr at room
317 temperature. The beads were washed with MIB 3 times and then eluted by 50 μ M SS-31. The
318 eluates were boiled with LDS protein loading buffer (Thermo, NP0008) and loaded on NuPAGE
319 for gel electrophoresis and Western blotting with antibody to ANT1 (Abcam, ab102032, 1:3000).
320 In some experiments, after electrophoresis, gels were silver stained using a Pierce Silver Stain
321 Kit (Thermo, #24612).

322 **Native coomassie blue staining and blotting.** Mitochondria from mouse hearts were isolated
323 as described previously (51). Mitochondria (100 μ g) were solubilized in 4x NativePAGE Sample
324 Buffer containing 5% digitonin and 5% coomassie blue G-250. The samples were loaded on
325 NativePAGE Novex 3-12% Gel and run at 100 V for 1 hr, then at 300 V for 2 hr. For coomassie
326 blue staining, gels were stained with 0.1 % Coomassie Brilliant Blue overnight and destained
327 with destaining solution (H₂O: Methanol: Acetic Acid = 5:4:1) 5 times at 20 min intervals. For
328 native blotting, gels were transferred to PVDF membranes at 25 V in 4 °C overnight and
329 incubated with ATP5a antibody (Abcam, ab14748, 1:3000), followed by anti-mouse secondary
330 antibody.

331 **Perfused mouse heart confocal imaging.** mt-cpYFP transgenic mice were anesthetized with
332 pentobarbital (150mg/kg). The heart was removed, cannulated via the ascending aorta, and put
333 on a modified perfusion system and in a custom made chamber on the confocal stage as
334 previously reported (48, 52). The perfusion was maintained under a constant flow (~2 mL/min)
335 with O₂/CO₂-bubbled KHB solution (in mM: 118 NaCl, 0.5 EDTA, 10 D-glucose, 5.3 KCl, 1.2
336 MgCl₂, 25 NaHCO₃, 0.5 Pyruvate, and 2 CaCl₂, pH 7.4) at 37 °C. To minimize motion artifact
337 during imaging, 10 μ M (-)-Blebbistatin (Toronto Research Chemicals) was included. During
338 imaging, the left ventricle was gently pressed to further suppress motion artifact. Mitoflashes
339 were imaged using the procedure described above.

340 **Data statistics.**

341 Data are shown as mean \pm SEM. One-way ANOVA was used for experiments with more than 2
342 groups, followed by Tukey's post hoc analysis. P < 0.05 was considered statistically significant.

343

344 **Conflict of interest**

345 Dr. Szeto Hazel has served as consultants to Stealth Biotherapeutics.

346

347 **Acknowledgements**

348 We thank Drs. Mariya Sweetwyne, Ying Ann Chiao, Martin Brand, Michael MacCoss and
349 Gaomin Feng for technical support and helpful discussions and the services of the W. M. Keck
350 Microscopy Center at the University of Washington. SS-31 (elamipretide) was kindly provided by
351 Stealth Biotherapeutics (Newton MA).

352 **Source of Funding**

353 This work was supported by NIA P01AG001751 and R56AG055114 to P.S.R., HL114760,
354 HL137266 and AHA 18EIA33900041 to W. W., and a Glenn Foundation for Medical Research
355 Postdoctoral Fellowship and AHA 19CDA34660311 to H.Z.

356

357 **Figure Legends**

358 Fig. 1: SS-31 alleviates the excessive mitochondrial proton leak of cardiomyocytes from 24 mo
359 old mice. (A) Representative Seahorse Assay traces of cardiomyocytes isolated from untreated
360 young and old mice, then exposed or not to 100nM SS-31 for 2 hr in vitro. Aging increased
361 basal respiration (C), which was attributable to the augmentation of proton leak (B), but did not
362 affect maximal respiration (D). (E) SS-31 improved the respiratory control ratio (RCR) in old
363 cardiomyocytes. ANT1 inhibitors BKA (10 μ M) and CAT (20 μ M) 2 hr treatment decreased the
364 proton leak (B) and basal respiration (C) but also decreased maximal respiration (D) and RCR
365 (E) in old cardiomyocytes. N=7-26 in each group *P < 0.05 vs. young, #P < 0.05 vs. old controls.

366

367 Fig. 2: SS-31 restores the resistance of cardiomyocytes from old mice to proton entry into the
368 mitochondrial matrix during external pH gradient stress. (A) saponin (50 μ g/ml) permeabilized
369 cardiomyocytes expressing mt-cpYFP were exposed to progressively lower external pH. Proton
370 permeability of old mitochondria was greater than that of young mitochondria, but preincubation
371 of old cells with 10 μ M SS-31 for 3 days enhanced the mitochondrial inner membrane resistance
372 to the pH stress. The arrows indicate the changes of pH. (B) Quantitation of the SS-31
373 treatment effect on the mitochondrial matrix cpYFP ratio at pH 5.3. The data are from 7-8 min
374 after the pH was adjusted to 5.3. (C) SS-31 decreased the rate of cpYFP 488/405 ratio drop at
375 pH 6.9. The rate is calculated as indicated in Supplemental Figure 4. The time dependence (D)
376 and dose dependence (E) of SS-31 protection of mitochondrial resistance to pH gradient stress
377 are shown. After cardiomyocyte permeabilization, 10 μ M SS-31 was added for the times shown
378 in (D) or at the doses shown in (E) for 30 minutes, followed by pH stress. N=4 - 18 in each
379 group *: P < 0.05 vs Young, #: P < 0.05 vs Old.

380

381 Fig. 3: ANT1 inhibitors restore resistance to proton leak in old cardiomyocytes. ANT1 inhibitors
382 10 μ M BKA and 20 μ M CAT, but not 50 μ M Genipin (UCP2 inhibitor) or 1 μ M OA (ATPase
383 inhibitor), protected the mitochondrial matrix from decreased pH after exposure to external pH
384 5.3 (A) and reduced the rate of 488/405 decline after exposure to pH 6.9 (B). BKA, CAT,
385 Genipin, or OA were added immediately after the mitochondria permeabilization. N=4-14 in
386 each group *P < 0.05 vs Young, #P < 0.05 vs Old.

387

388 Fig. 4: SS-31 attenuates excessive mitoflash activity in aged cardiomyocytes. (A-C) Mitoflash
389 events within the regions shown in the red boxes took place at the times shown by vertical bars
390 during the 100 sec scanning time in the representative cardiomyocytes from young (A), old (B)

391 and old+SS-31 (C) hearts. (D) The rate of mitoflash activity was increased in old
392 cardiomyocytes compared to young, but 1 hour SS-31, BKA (10 μ M) and CAT (20 μ M)
393 treatments decreased the mitoflash frequency in old cells to or below that of young cells. N =
394 26-88 cells from 4-8 rats. (E) JC-1 red to green fluorescence ratio, indicative of mitochondrial
395 membrane potential, in cells from young and old mice and old cells from mice treated with SS-
396 31 (10 μ M for 12 hours). N= 17-65 cells. (F) Mitochondrial ROS production measured by the
397 fluorescence ratio of MitoSOX (5 μ M, excitation 540 nm, emission >560 nm) to Mitotracker
398 green (200 nM, excitation 488 nm, emission 505-530 nm). N=13-26 cells. *P < 0.05 vs young.
399 #P < 0.05 vs old.

400

401 Fig. 5: SS-31 reverses the increased speed of mPTP opening in aged cardiomyocytes. (A) A
402 typical image shows 1 Hz line-scanning photo-excitation induced mPTP opening in a
403 cardiomyocyte loaded with the mitochondrial membrane potential ($\Delta\psi_m$) dye TMRM. The
404 sudden decline of TMRM fluorescence with time (rightward) indicates mPTP opening and $\Delta\psi_m$
405 loss. (B) 1 hour SS-31 and BKA, but not CAT treatments protect the photo-excitation induced
406 mPTP opening. Quantification of time to mPTP opening from 338-419 mitochondria from 16-18
407 cells isolated from 3 mice in each group. *P < 0.01 vs young, #P < 0.01 vs old.

408

409 Fig. 6: SS-31 interacts with ANT1 and stabilizes the ATP synthasome. (A, B) Biotin-SS-31
410 pulldown shows the association of biotin-SS-31 to ANT1. Free SS-31 competes with this
411 interaction, while BKA and CAT inhibit the interaction of biotin-SS-31 with ANT1. Panel A shows
412 a representative Western blot. (C) Coomassie blue staining of isolated mitochondria in a native
413 gel. (D, E) Native Gel blotting shows that 10 μ M SS-31 stabilizes the mitochondrial synthasome
414 (Syn) in isolated mitochondria. The Syn is highlighted in the red box. The Syn and ATPase
415 Dimer (D) and Monomer (M) were labeled using anti-ATP5A.

416

417 Fig. 7: Schematic of the mechanism of SS-31 protection of proton leak and rejuvenation of
418 mitochondrial function. Due to increased mitochondrial proton leak, the mitochondria work
419 harder to maintain ATP production, and thus the work load is increased in the aged heart.

420

421 Supplemental Fig. 1: SS-31 reaches its inhibitory effect on proton leak suppression at low
422 concentrations. SS-31 decreased the mitochondrial proton leak. N=7-24 in each group *P < 0.05
423 vs. young, #P < 0.05 vs. old controls.

424

425 Supplemental Fig. 2: pH calibration of mt-cpYFP in adult cardiac myocytes. 10 μ M Nigericin was
426 added to the mitochondrial permeabilization buffer. (A) shows the ratio of 488/405 (normalized
427 to that of the value at pH=7.5) as the pH is gradually lowered. The ratio of 488/405 reaches the
428 lowest point at pH 6.0, followed by a small increase starting at pH 5.5, consistent with the known
429 pH response of this dye (23). (B) shows the emission spectra of mt-cpYFP pH 8.0, 6.0 and 4.5
430 when excited at 488 nm (C) shows the emission spectra of mt-cpYFP pH 8.0, 6.0 and 4.5 when
431 excited at 405nm. The 488 nm excitation is sensitive to the pH change but the 405 nm excitation
432 is much less pH dependent.

433

434 Supplemental Fig. 3: Typical image of the effects of pH gradient stress on permeabilized
435 cardiomyocyte mt-cpYFP fluorescence. (A) Young, (B) Old, (C) Old+SS31 (10 μ M, 3 days)

436 visualized after exposure of the cells to pH 7.5 and, later, to pH 5.3. The excitation is 488 nm
437 and collection is at 505-730nm.

438

439 Supplemental Fig. 4: Method of quantitation of the slope of mt-cpYFP fluorescence ratio change
440 after permeabilized cells are exposed to external pH 6.9. The trace is from old cardiomyocytes.

441

442 Supplemental Fig. 5: Aging effect on ANT1 and UCP2 cardiac protein abundance. Aging
443 slightly, but significantly decreases ANT1 levels in the heart. Western blot of ANT1 (A, C) and
444 UCP2 (B, D). n=6/group. *P < 0.05 vs young. The total protein loading control was stained with
445 MemCode Reversible Protein Stain Kit for Polyvinylidene difluoride Membranes (Pierce,
446 Rockford, IL).

447

448 Supplemental Fig. 6: Increased mitochondrial flash activity in the intact perfused aged heart. (A)
449 Typical images from the young (upper panel) and old (lower panel) hearts. (B) Statistical
450 analysis of mitoflash frequency in the analyzed regions indicated by the red boxes in panel A.
451 Young: N=19 regions from 3 mice. Old: N=16 regions from 4 mice. *P < 0.05 vs Young.

452

453 Supplemental Fig. 7: The total protein loading control for the Native gel blot shown in Figure 6D.

454

455 Supplemental Fig. 8: Silver staining of the Biotin-SS-31 pulldown of Figure 6A. The great
456 majority of bands present in the input are not present in the biotin-SS-31 pulldown; those that
457 are show suppression by SS-31 competition.

458

459 Reference

- 460 1. Dai DF, Chiao YA, Marcinek DJ, Szeto HH, & Rabinovitch PS (2014) Mitochondrial oxidative stress
461 in aging and healthspan. *Longev Healthspan* 3:6.
- 462 2. Lesnefsky EJ, Chen Q, & Hoppel CL (2016) Mitochondrial Metabolism in Aging Heart. *Circ Res*
463 118(10):1593-1611.
- 464 3. Perez VI, *et al.* (2009) Is the oxidative stress theory of aging dead? *Biochim Biophys Acta*
465 1790(10):1005-1014.
- 466 4. Brand MD (2005) The efficiency and plasticity of mitochondrial energy transduction. *Biochem*
467 *Soc Trans* 33(Pt 5):897-904.
- 468 5. Rolfe DF & Brand MD (1996) Contribution of mitochondrial proton leak to skeletal muscle
469 respiration and to standard metabolic rate. *Am J Physiol* 271(4 Pt 1):C1380-1389.
- 470 6. Divakaruni AS & Brand MD (2011) The regulation and physiology of mitochondrial proton leak.
471 *Physiology (Bethesda)* 26(3):192-205.
- 472 7. Brand MD, *et al.* (2005) The basal proton conductance of mitochondria depends on adenine
473 nucleotide translocase content. *Biochem J* 392(Pt 2):353-362.
- 474 8. Harper ME, Monemdjou S, Ramsey JJ, & Weindruch R (1998) Age-related increase in
475 mitochondrial proton leak and decrease in ATP turnover reactions in mouse hepatocytes. *Am J*
476 *Physiol* 275(2 Pt 1):E197-206.
- 477 9. Serviddio G, *et al.* (2007) Bioenergetics in aging: mitochondrial proton leak in aging rat liver,
478 kidney and heart. *Redox Rep* 12(1):91-95.

- 479 10. Birk AV, *et al.* (2013) The mitochondrial-targeted compound SS-31 re-energizes ischemic
480 mitochondria by interacting with cardiolipin. *J Am Soc Nephrol* 24(8):1250-1261.
- 481 11. Szeto HH (2014) First-in-class cardiolipin-protective compound as a therapeutic agent to restore
482 mitochondrial bioenergetics. *Br J Pharmacol* 171(8):2029-2050.
- 483 12. Szeto HH & Birk AV (2014) Serendipity and the discovery of novel compounds that restore
484 mitochondrial plasticity. *Clin Pharmacol Ther* 96(6):672-683.
- 485 13. Szeto HH (2008) Mitochondria-targeted cytoprotective peptides for ischemia-reperfusion injury.
486 *Antioxid Redox Signal* 10(3):601-619.
- 487 14. Cho J, *et al.* (2007) Potent mitochondria-targeted peptides reduce myocardial infarction in rats.
488 *Coron Artery Dis* 18(3):215-220.
- 489 15. Dai DF, *et al.* (2013) Global proteomics and pathway analysis of pressure-overload-induced heart
490 failure and its attenuation by mitochondrial-targeted peptides. *Circ Heart Fail* 6(5):1067-1076.
- 491 16. Yang L, *et al.* (2009) Mitochondria targeted peptides protect against 1-methyl-4-phenyl-1,2,3,6-
492 tetrahydropyridine neurotoxicity. *Antioxid Redox Signal* 11(9):2095-2104.
- 493 17. Anderson EJ, *et al.* (2009) Mitochondrial H₂O₂ emission and cellular redox state link excess fat
494 intake to insulin resistance in both rodents and humans. *J Clin Invest* 119(3):573-581.
- 495 18. Sweetwyne MT, *et al.* (2017) The mitochondrial-targeted peptide, SS-31, improves glomerular
496 architecture in mice of advanced age. *Kidney Int* 91(5):1126-1145.
- 497 19. Hao ZH, *et al.* (2017) SS31 ameliorates age-related activation of NF-kappaB signaling in senile
498 mice model, SAMP8. *Oncotarget* 8(2):1983-1992.
- 499 20. Siegel MP, *et al.* (2013) Mitochondrial-targeted peptide rapidly improves mitochondrial
500 energetics and skeletal muscle performance in aged mice. *Aging Cell* 12(5):763-771.
- 501 21. Chiao YA, *et al.* (2020) Late-life restoration of mitochondrial function reverses cardiac
502 dysfunction in old mice. *BioRxiv* <https://doi.org/10.1101/2020.01.02.893008>
- 503 22. Wang W, *et al.* (2008) Superoxide flashes in single mitochondria. *Cell* 134(2):279-290.
- 504 23. Wei-LaPierre L, *et al.* (2013) Respective contribution of mitochondrial superoxide and pH to
505 mitochondria-targeted circularly permuted yellow fluorescent protein (mt-cpYFP) flash activity. *J*
506 *Biol Chem* 288(15):10567-10577.
- 507 24. Demarex N & Schwarzlander M (2016) Mitochondrial Flashes: Dump Superoxide and Dance
508 with Protons Now. *Antioxid Redox Signal* 25(9):550-551.
- 509 25. Wang W, *et al.* (2016) Mitochondrial Flash: Integrative Reactive Oxygen Species and pH Signals
510 in Cell and Organelle Biology. *Antioxid Redox Signal* 25(9):534-549.
- 511 26. Bertholet AM, *et al.* (2019) H(+) transport is an integral function of the mitochondrial ADP/ATP
512 carrier. *Nature* 571(7766):515-520.
- 513 27. Ruprecht JJ, *et al.* (2019) The Molecular Mechanism of Transport by the Mitochondrial ADP/ATP
514 Carrier. *Cell* 176(3):435-447 e415.
- 515 28. Pebay-Peyroula E, *et al.* (2003) Structure of mitochondrial ADP/ATP carrier in complex with
516 carboxyatractyloside. *Nature* 426(6962):39-44.
- 517 29. Karch J, *et al.* (2019) Inhibition of mitochondrial permeability transition by deletion of the ANT
518 family and CypD. *Sci Adv* 5(8):eaaw4597.
- 519 30. Zhang M, *et al.* (2015) Remodeling of Mitochondrial Flashes in Muscular Development and
520 Dystrophy in Zebrafish. *PLoS One* 10(7):e0132567.
- 521 31. Shen EZ, *et al.* (2014) Mitoflash frequency in early adulthood predicts lifespan in *Caenorhabditis*
522 *elegans*. *Nature* 508(7494):128-132.
- 523 32. Feng G, Liu B, Hou T, Wang X, & Cheng H (2017) Mitochondrial Flashes: Elemental Signaling
524 Events in Eukaryotic Cells. *Handb Exp Pharmacol* 240:403-422.
- 525 33. Hou T, Wang X, Ma Q, & Cheng H (2014) Mitochondrial flashes: new insights into mitochondrial
526 ROS signalling and beyond. *J Physiol* 592(17):3703-3713.

- 527 34. Wang W, Zhang H, & Cheng H (2016) Mitochondrial flashes: From indicator characterization to
528 in vivo imaging. *Methods* 109:12-20.
- 529 35. Wang X, *et al.* (2016) Protons Trigger Mitochondrial Flashes. *Biophys J* 111(2):386-394.
- 530 36. Zorov DB, Filburn CR, Klotz LO, Zweier JL, & Sollott SJ (2000) Reactive oxygen species (ROS)-
531 induced ROS release: a new phenomenon accompanying induction of the mitochondrial
532 permeability transition in cardiac myocytes. *J Exp Med* 192(7):1001-1014.
- 533 37. Hafner AV, *et al.* (2010) Regulation of the mPTP by SIRT3-mediated deacetylation of CypD at
534 lysine 166 suppresses age-related cardiac hypertrophy. *Aging (Albany NY)* 2(12):914-923.
- 535 38. Halestrap AP, Woodfield KY, & Connern CP (1997) Oxidative stress, thiol reagents, and
536 membrane potential modulate the mitochondrial permeability transition by affecting nucleotide
537 binding to the adenine nucleotide translocase. *J Biol Chem* 272(6):3346-3354.
- 538 39. Johnson SC, *et al.* (2013) mTOR inhibition alleviates mitochondrial disease in a mouse model of
539 Leigh syndrome. *Science* 342(6165):1524-1528.
- 540 40. Vignais PV, Douce R, Lauquin GJ, & Vignais PM (1976) Binding of radioactively labeled
541 carboxyatractyloside, atractyloside and bongkreikic acid to the ADP translocator of potato
542 mitochondria. *Biochim Biophys Acta* 440(3):688-696.
- 543 41. Ko YH, Delannoy M, Hullihen J, Chiu W, & Pedersen PL (2003) Mitochondrial ATP synthasome.
544 Cristae-enriched membranes and a multiwell detergent screening assay yield dispersed single
545 complexes containing the ATP synthase and carriers for Pi and ADP/ATP. *J Biol Chem*
546 278(14):12305-12309.
- 547 42. Olgar Y, Tuncay E, & Turan B (2019) Mitochondria-Targeting Antioxidant Provides
548 Cardioprotection through Regulation of Cytosolic and Mitochondrial Zn(2+) Levels with Re-
549 Distribution of Zn(2+)-Transporters in Aged Rat Cardiomyocytes. *Int J Mol Sci* 20(15).
- 550 43. Chavez JD, *et al.* (2019) Mitochondrial protein interaction landscape of SS-31. *BioRxiv*
551 <https://doi.org/10.1101/739128>
- 552 44. Mitchell W, *et al.* (2019) Molecular Mechanism of Action of Mitochondrial Therapeutic SS-31
553 (Elamipretide): Membrane Interactions and Effects on Surface Electrostatics. *BioRxiv*
554 <https://doi.org/10.1101/735001>
- 555 45. Karaa A, *et al.* (2018) Randomized dose-escalation trial of elamipretide in adults with primary
556 mitochondrial myopathy. *Neurology* 90(14):e1212-e1221.
- 557 46. Brand MD (2000) Uncoupling to survive? The role of mitochondrial inefficiency in ageing. *Exp*
558 *Gerontol* 35(6-7):811-820.
- 559 47. Zhang H, *et al.* (2013) Beta-adrenergic-stimulated L-type channel Ca(2)+ entry mediates hypoxic
560 Ca(2)+ overload in intact heart. *J Mol Cell Cardiol* 65:51-58.
- 561 48. Zhang H, *et al.* (2017) A novel fission-independent role of dynamin-related protein 1 in cardiac
562 mitochondrial respiration. *Cardiovasc Res* 113(2):160-170.
- 563 49. Lukyanenko V & Gyorke S (1999) Ca²⁺ sparks and Ca²⁺ waves in saponin-permeabilized rat
564 ventricular myocytes. *J Physiol* 521 Pt 3:575-585.
- 565 50. Chiao YA, *et al.* (2016) Rapamycin transiently induces mitochondrial remodeling to reprogram
566 energy metabolism in old hearts. *Aging (Albany NY)* 8(2):314-327.
- 567 51. Marcu R, Neeley CK, Karamanlidis G, & Hawkins BJ (2012) Multi-parameter measurement of the
568 permeability transition pore opening in isolated mouse heart mitochondria. *J Vis Exp* (67).
- 569 52. Zhang H, *et al.* (2018) Heart specific knockout of Ndufs4 ameliorates ischemia reperfusion injury.
570 *J Mol Cell Cardiol* 123:38-45.

571

572

Fig. 1: SS-31 alleviates the excessive mitochondrial proton leak in the old cardiomyocytes.

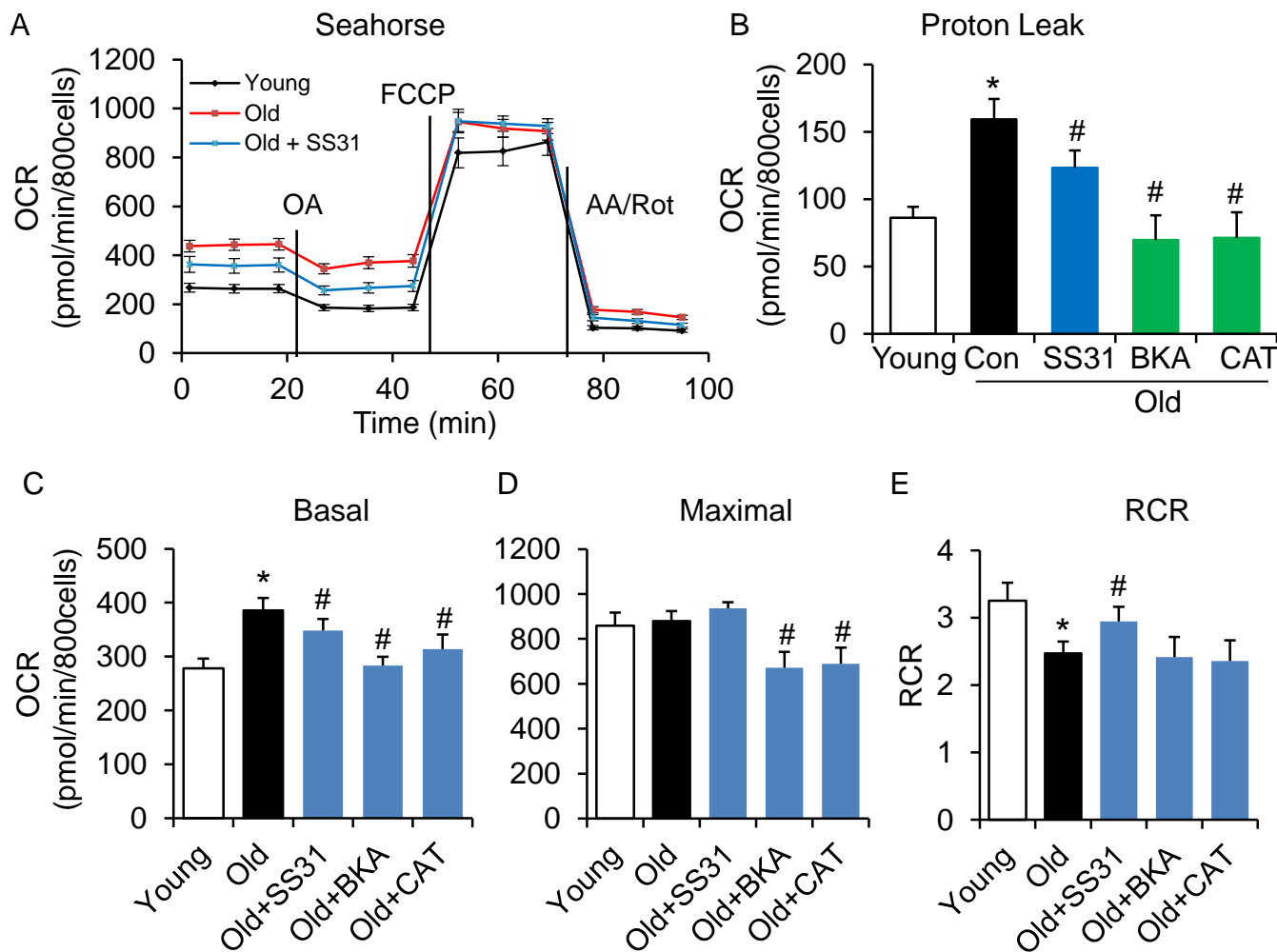


Fig. 2: SS31 restores the resistance to external pH gradient stress in the old cardiomyocytes.

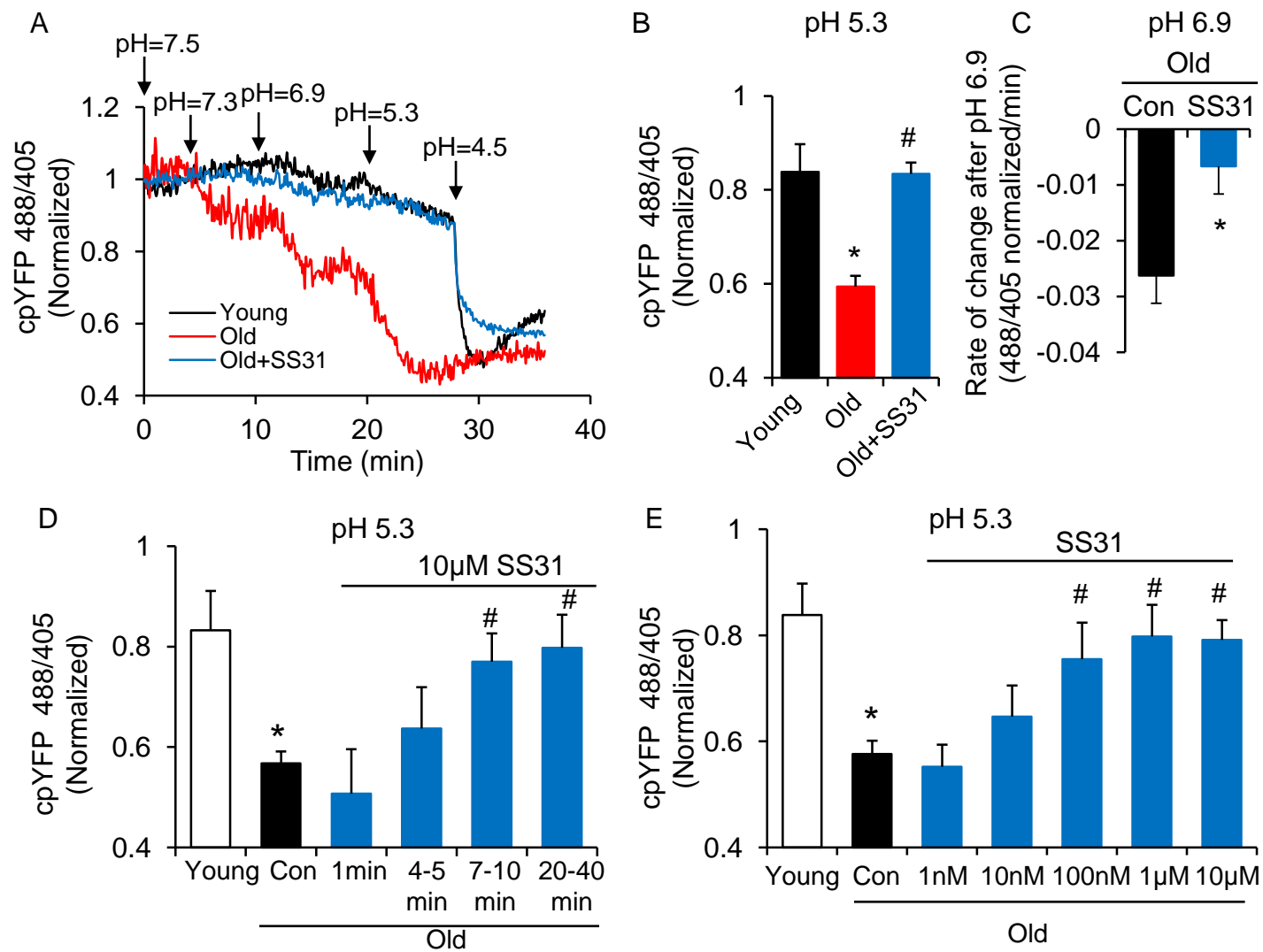


Fig. 3: ANT1 inhibitors restore resistance to proton leak in old cardiomyocytes.

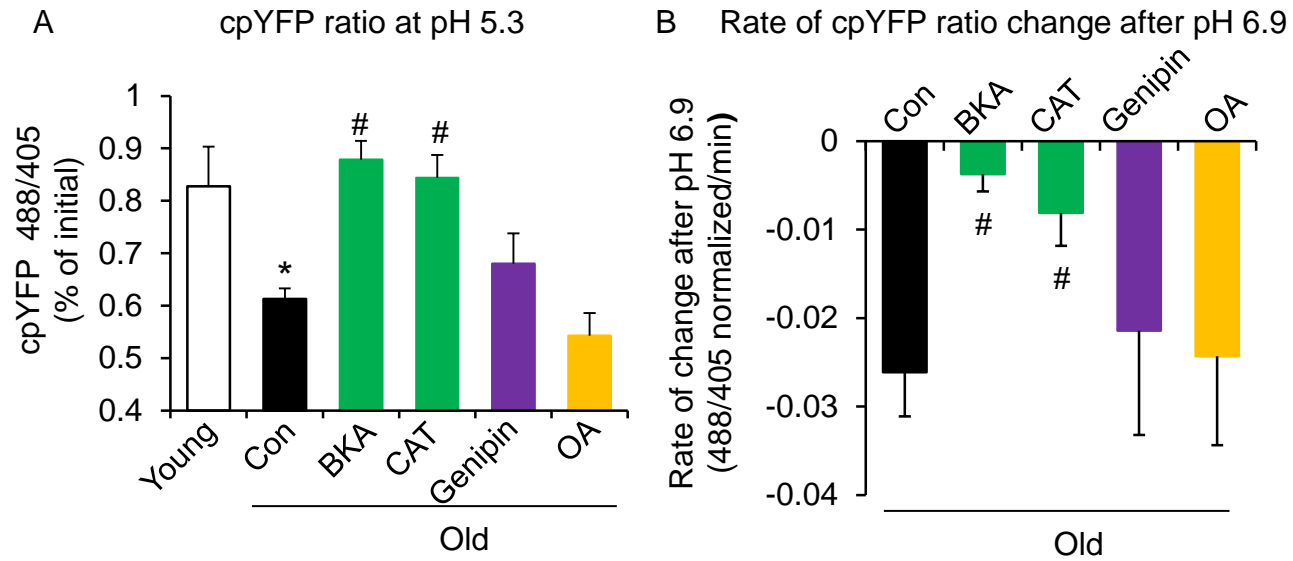


Fig. 4: SS31 attenuates the excessive mitoflash activity in aged cardiomyocytes

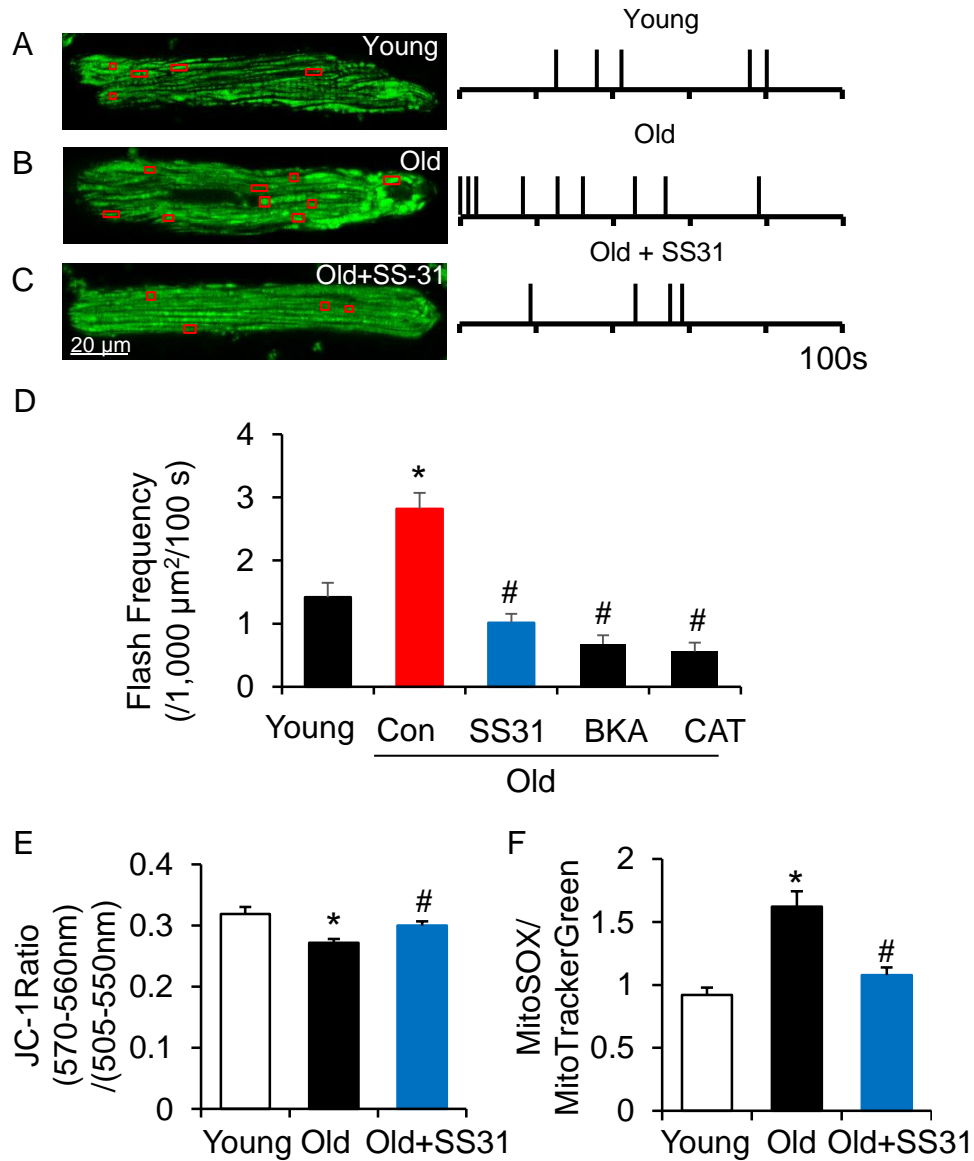


Fig. 5: SS-31 reverses the increased mPTP opening in aged cardiomyocytes.

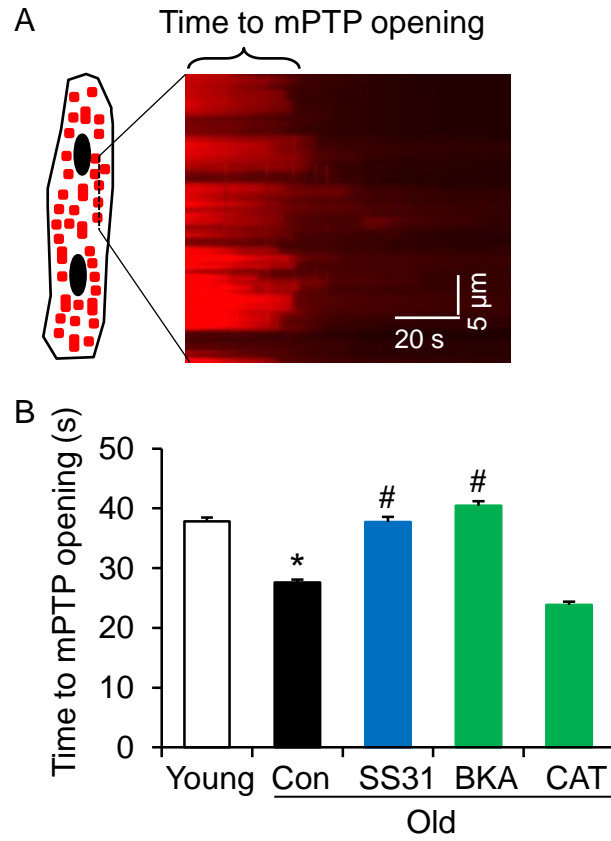


Fig. 6: SS31 associates directly with ANT1 and stabilizing the ATP synthasome

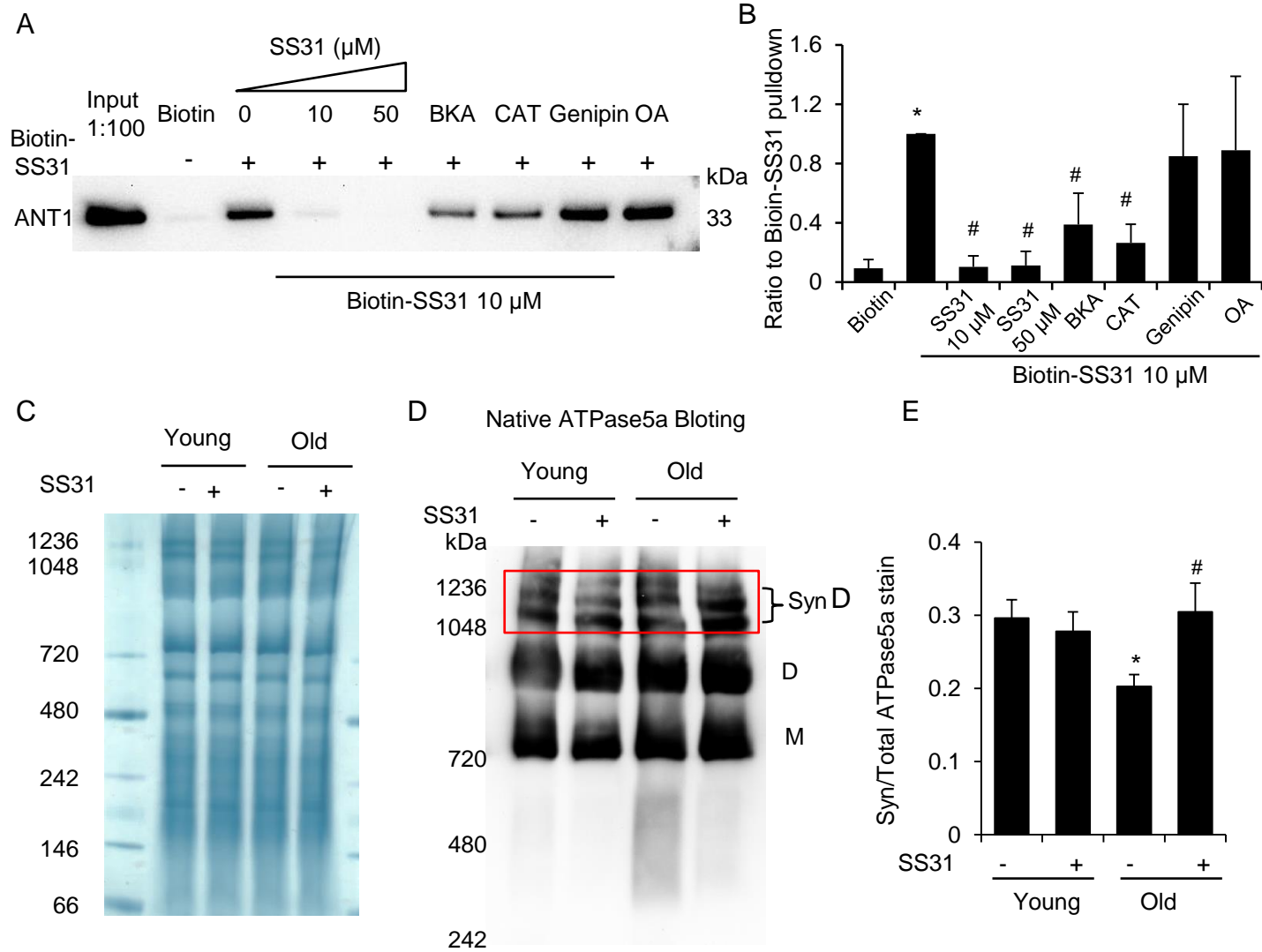
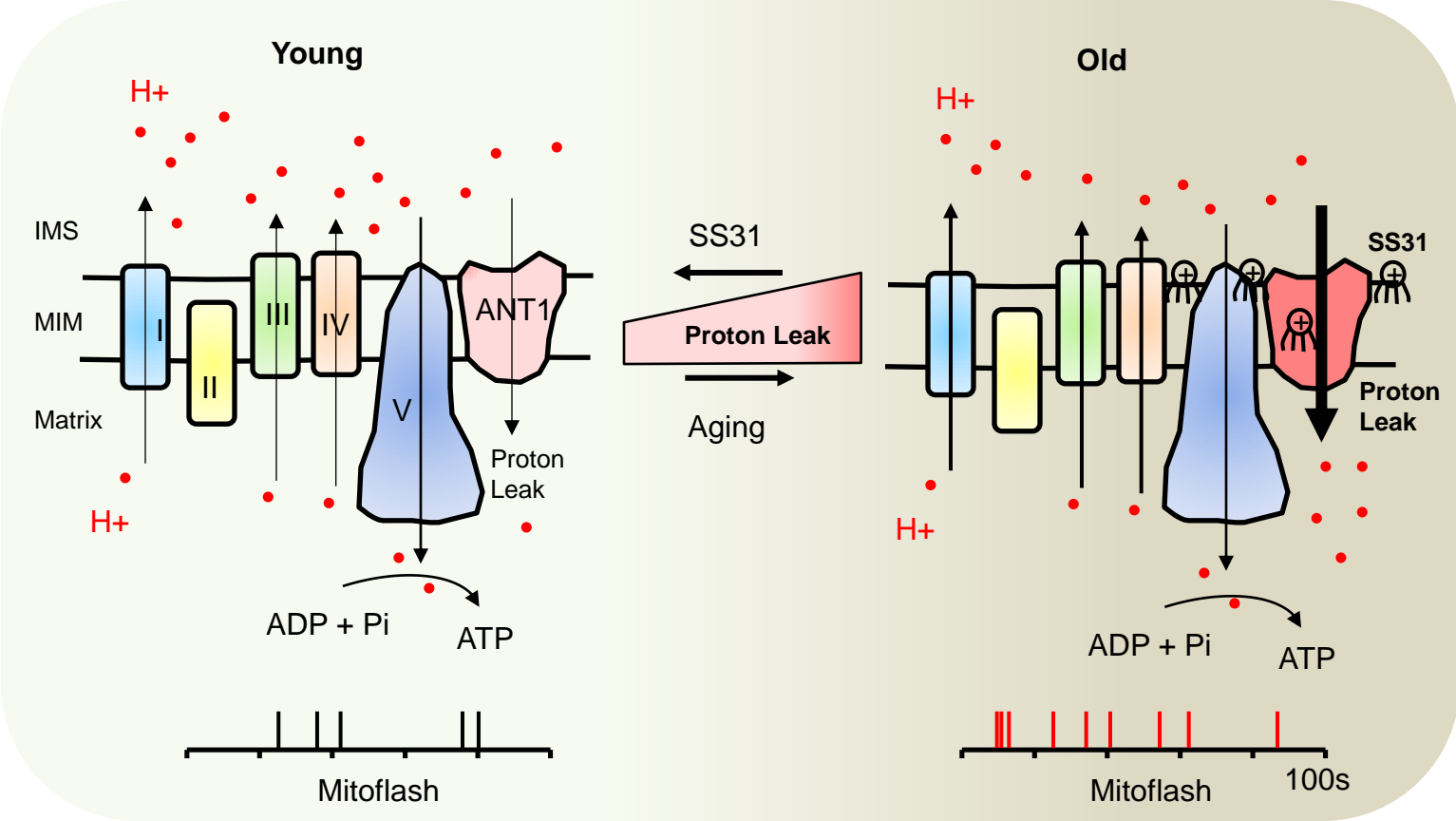



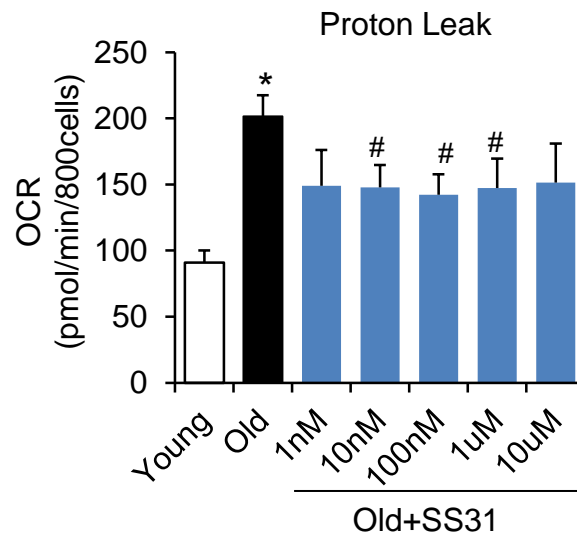
Fig. 7: Diagram of SS-31 prevent proton leak and rejuvenated mitochondrial function



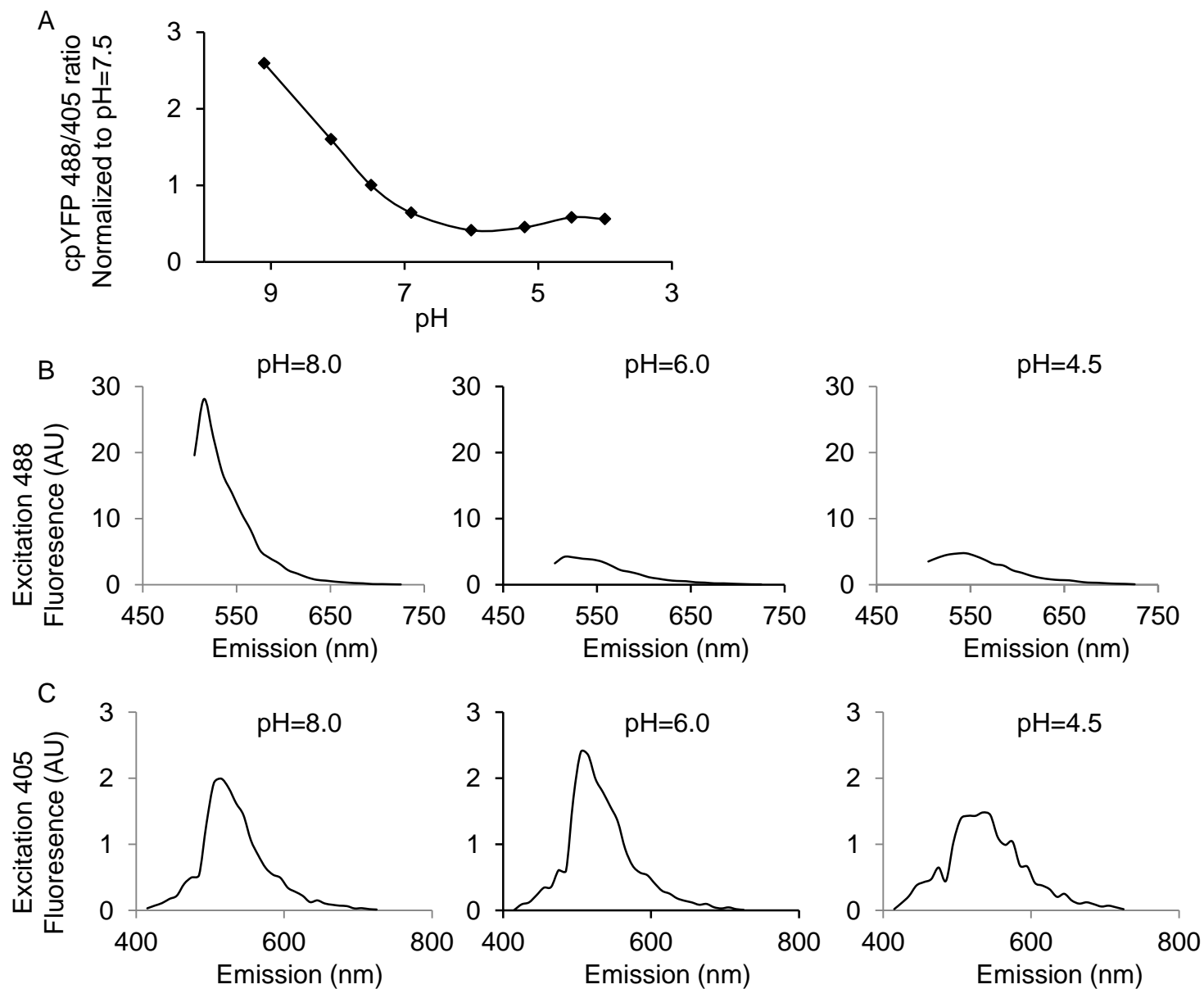
 SS31

IMS: Intermembrane Space
MIM: Mitochondrial Inner Membrane

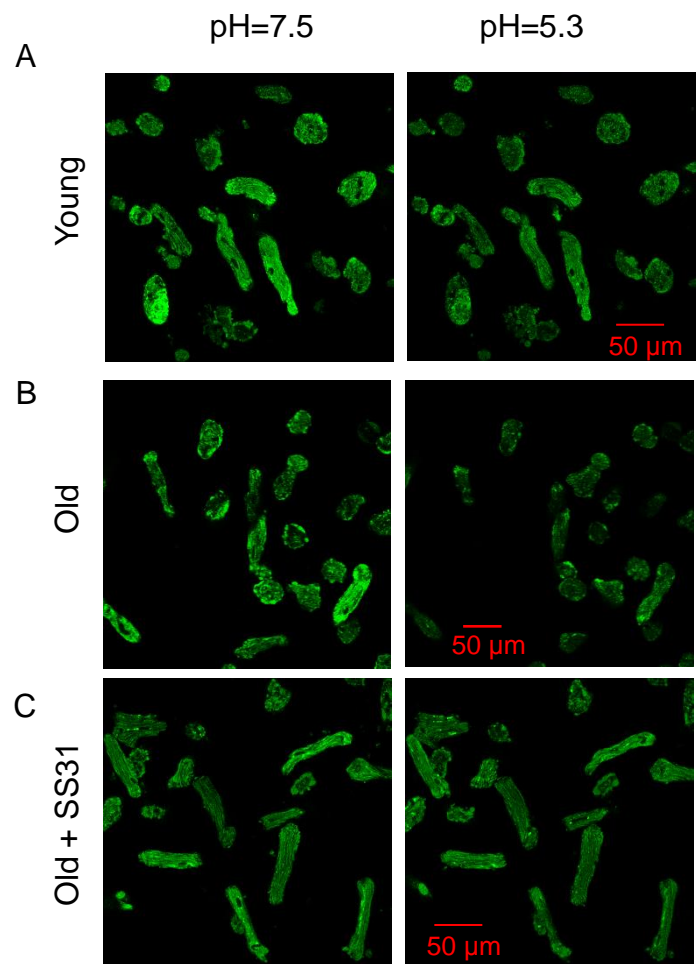
Supplemental Fig. 1: SS-31 reaches its inhibitory effect on proton leak suppression at low concentrations



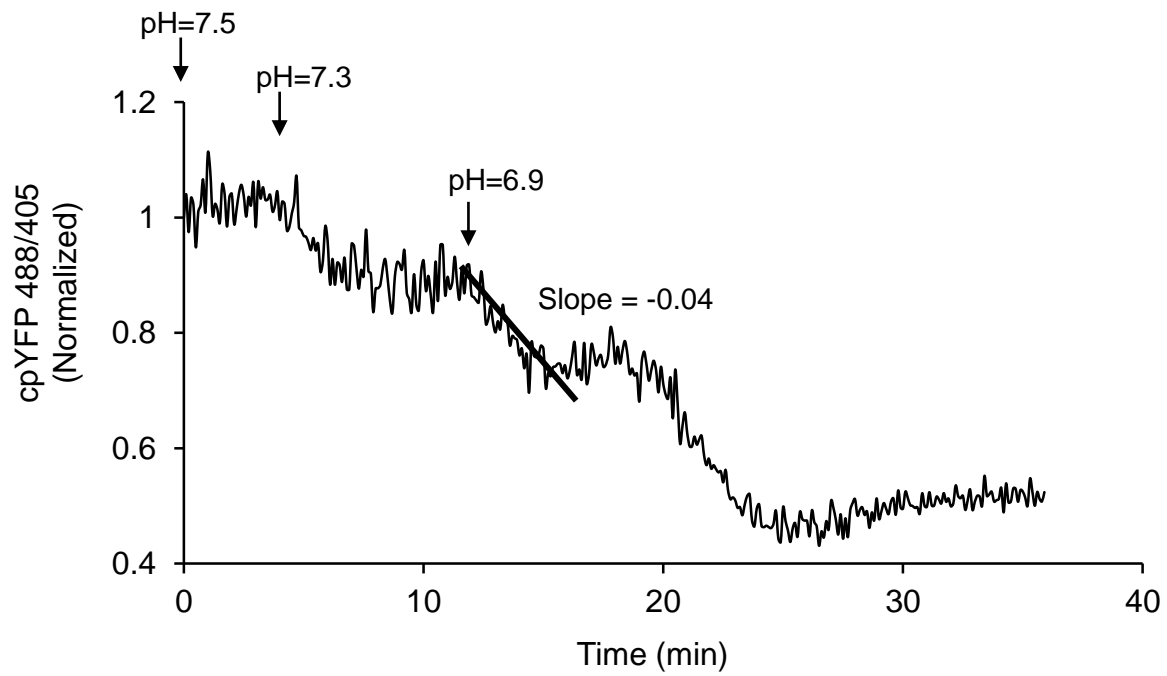
Supplemental Fig. 2: cpYFP fluorescent pH calibration



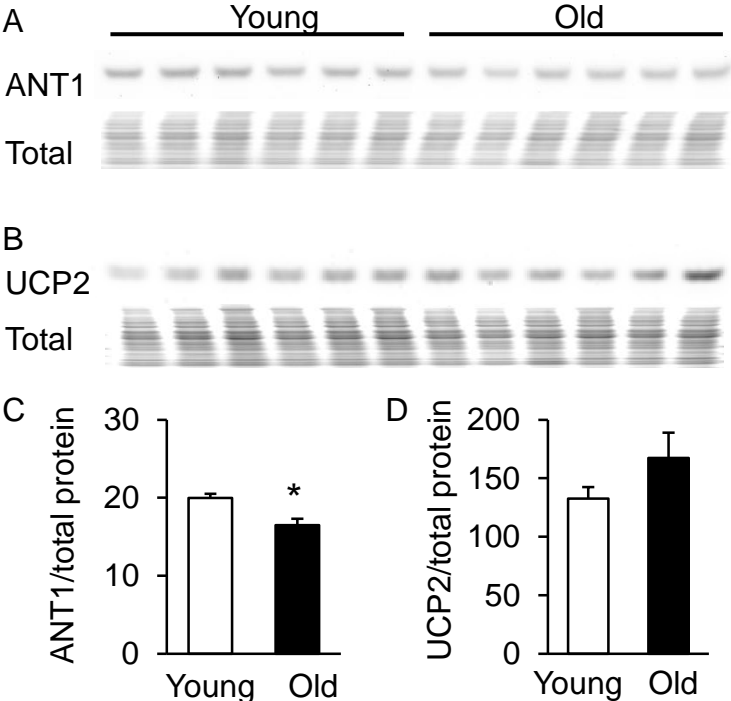
Supplemental Fig. 3: Typical image of pH gradient stress on permeabilized cardiomyocytes.



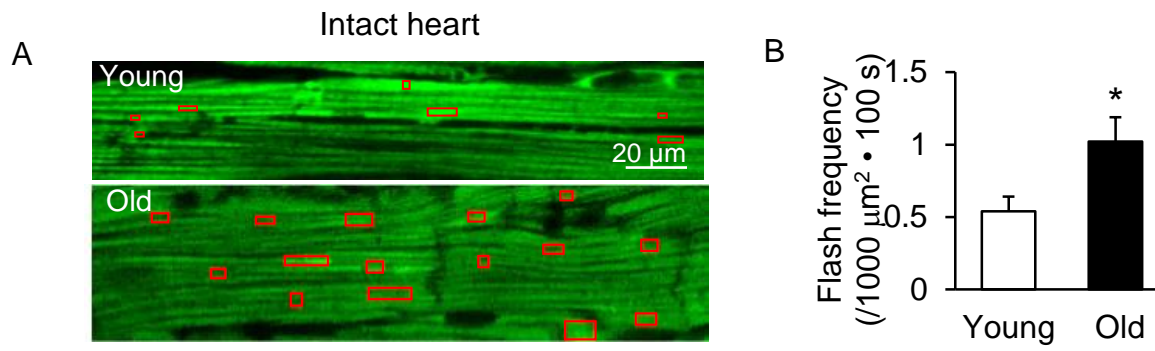
Supplemental Fig. 4: Mitochondrial pH reaches a plateau after a lower pH stress.



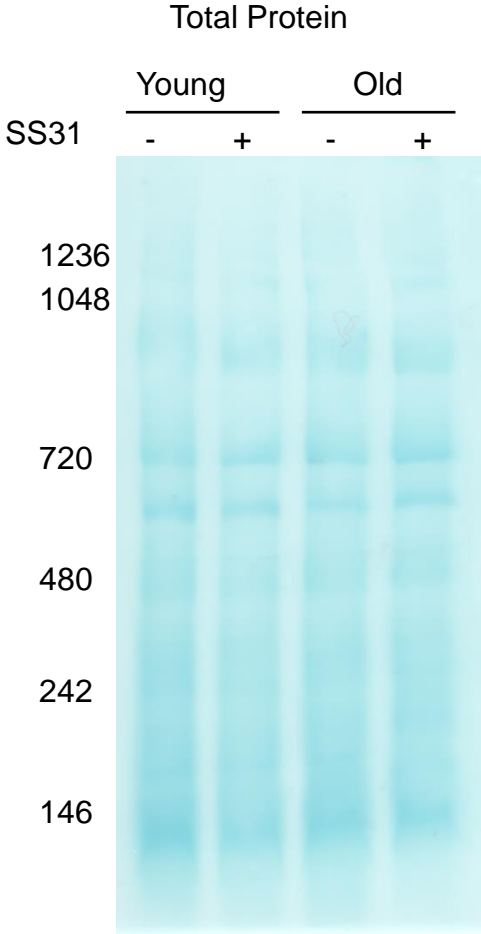
Supplemental Fig. 5: Aging effect on the proton leak proteins.



Supplemental Fig. 6: Increased mitochondrial flash in the aged intact heart.



Supplemental Fig. 7: Loading control of the Native gel bolting



Supplemental Fig. 8: Silver stain of Biotin-SS31 pulldown

